

Phase-transition oscillations induced by a strongly focused laser beam

Clémence Devailly,^{*} Caroline Crauste-Thibierge, Artyom Petrosyan, and Sergio Ciliberto
*Université de Lyon, Laboratoire de Physique, École Normale Supérieure de Lyon, CNRS UMR5672, 46, Allée d'Italie,
 69364 Lyon Cedex 07, France*

(Received 9 March 2015; revised manuscript received 21 July 2015; published 24 November 2015)

We report the observation of a surprising phenomenon consisting in an oscillating phase transition which appears in a binary mixture when this is enlightened by a strongly focused infrared laser beam. The mixture is poly-methyl-meth-acrylate (PMMA)–3-octanone, which has an upper critical solution temperature at $T_c = 306.6$ K and volume fraction $\phi_c = 12.8\%$ [Crauste *et al.*, [arXiv:1310.6720](https://arxiv.org/abs/1310.6720), 2013]. We describe the dynamical properties of the oscillations, which are produced by a competition between various effects: the local accumulation of PMMA produced by the laser beam, thermophoresis, and nonlinear diffusion. We show that the main properties of this kind of oscillations can be reproduced in the Landau theory for a binary mixture in which a local driving mechanism, simulating the laser beam, is introduced.

DOI: [10.1103/PhysRevE.92.052312](https://doi.org/10.1103/PhysRevE.92.052312)

PACS number(s): 64.75.Cd, 05.45.–a, 05.70.Ln, 64.60.an

I. INTRODUCTION

Phase transitions in binary mixtures are still a widely studied subject, specifically near the critical point where several interesting and not completely understood phenomena may appear, such as critical Casimir forces [1,2], confinement effects [3,4], and out-of-equilibrium dynamics after a quench. The perturbation of the binary mixtures by means of external fields is also an important subject of investigation [5]. For example, a laser can induce interesting phenomena in demixing binary mixtures because the radiation pressure can deform the interface between the two phases [6].

In Ref. [7] a focused infrared laser beam heated the medium initially in the homogeneous phase and caused a separation in the low critical solution temperature system. The local heating may induce thermophoretic forces which attract towards the laser beam one of the binary-mixture components [8]. Other forces like electrostriction can also be involved [9].

In this article, we report a phenomenon which consists in an oscillating phase transition induced by a constant illumination from an infrared laser beam in the heterogeneous region of an upper critical solution temperature (UCST) binary mixture. Oscillation phenomena in phase transition have already been reported in slow cooling UCST [10,11] but, as far as we know, never induced by a stationary laser illumination. After describing our experimental setup, we will present the results. Then we will show that a model, based on the Landau approach for binary mixture, reproduces this oscillatory phenomenon when a local pumping mechanism is introduced. The paper is organized as follows: in Sec. II we present the experimental setup. In Sec. III we describe the oscillatory phenomenon, and we discuss the possible physical mechanisms at the origin of this time-dependent behavior. In Sec. IV the model based on the mean field theory of phase transition is presented with the numerical results. We conclude in Sec. V.

II. EXPERIMENTAL SETUP

The medium is a binary mixture of poly-methyl-meth-acrylate (PMMA; Fluka, analytical standard for GPC) with

a molecular weight $M_w = 55900$ g/mol and a polydispersity $M_w/M_n = 1.035$ and 3-octanone (sup. 98%; both purchased from Sigma-Aldrich). This binary mixture presents an UCST [12] measured in Ref. [13] around $T_c = 306.6$ K and at the critical PMMA volume fraction $\phi_c = 12.8\%$. The phase diagram volume fraction-temperature presents a high-temperature homogeneous region and a low-temperature two-phase region with a polymer-rich and a polymer-poor phase. We prepare the sample, under a laminar flow hood, at different volume fractions by weighting the polymer before adding a volume of 3-octanone calculated from the density of the polymer $\rho_{\text{PMMA}} = 1.17$ given by the supplier. The solution is then mixed at 325 K over one night to ensure a good dissolution. The measured phase diagram (temperature T versus the volume fraction ϕ) of the PMMA–3-octanone mixture [13] is reproduced in Fig. 1. The simplest way to describe the coexistence curve $T(\phi_o)$ is to fit it by a parabolic curve $T(\phi_o) = T_c - \frac{b_0}{a_0}(\phi_o - \phi_c)^2$, where b_0 and a_0 are system-dependent constants. This is equivalent to modeling the system using the Ginzburg-Landau theory of phase transitions. For the polymer-solvent mixture this is not the more appropriate theory [14], but it is the simplest approximation and will be used in Sec. V to give more insight into the role of a local forcing on a phase transition.

The cell containing the sample is composed of a 1-mm-thick glass plate and by a cover slip separated by a 100 μm -thick polycarbonate sheet and glued with NOA 81 under UV light. The top glass plate has two apertures connected with two filling metallic tubes. To fill the cell, we heat all the materials (syringe, needle, cell) and the medium to avoid demixing during the filling. Then we close the two openings with a small amount of wax. Two metallic tubes prevent wax to be directly in contact with the mixture. We leave the cell for several hours at room temperature to let the medium demix properly. We obtained a cell containing two phases with typical size of the regions being around 20 μm to 200 μm . The filled cell is inserted in a microscope. Then the samples are left for several hours at room temperature to let the medium have a proper demixing. They are placed in glass cells inserted in a Leica microscope. A laser beam ($\lambda = 1064$ nm) is focused on each sample [15]. A white light source is also used to illuminate the sample; this light is collected by the $\times 63$ objective, and the sample is observed with a fast camera (Mikrotron MC1310). The optics

^{*}Present address: School of Physics and Astronomy, University of Edinburgh, Edinburgh, EH9 3FD, United Kingdom.

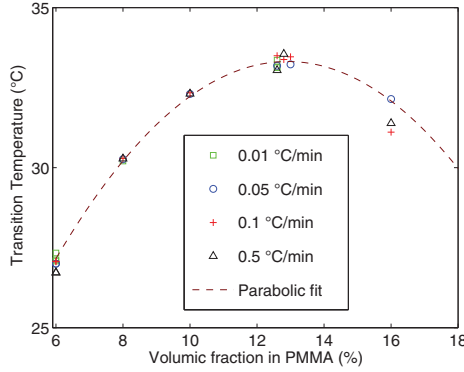


FIG. 1. (Color online) PMMA-octanone coexistence diagram obtained from cloud point measurements [13] performed at different fixed concentration ϕ_o by decreasing the temperature at various rates. The parabolic fit $T_{eq}(\phi_o)$ is done using the data obtained at the two slowest ramp rates.

of the setup is given in Ref. [14]. The laser power is calibrated by measuring the power of the laser beam just before the objective. Thus, it is not exactly the value of the intensity in the cell. The attenuation of the microscope objective is about 70% at 1064 nm. At room temperature, the mixture at PMMA volume fraction $\phi = \phi_c = 12.8\%$ is in the two-phase region. So we can see droplets of one phase in the other one. After a long time, these droplets coalesce. Nevertheless, the medium is thin enough to avoid the segregation of the two phases due to gravity. At $\phi = 12.8\%$, these droplets are steady.

III. OSCILLATORY PHENOMENON

When the laser is switched on, a droplet of one phase appears at the focal point of the laser (see Fig. 2). This droplet size increases until a maximum radius is reached, and then it decreases. When the droplet disappears, another one appears close to the vanishing one, and another cycle of growth and decrease begins. This phenomenon could persist for several oscillations (between 1 and 20). When it stops, we observe some dense PMMA aggregates on the bottom of the cell. Sometimes the phenomenon stops because we place the laser too close to an existing droplet, and the created one coalesces with an existing one. The oscillatory phenomenon appears also in a sample at $\phi = 2\%$ of PMMA, that is, a noncritical mixture. Moreover, in this solution, the number of droplets is less important, and droplets are more mobile due to a smaller viscosity of the sample. These mobile droplets can be easily trapped by the focused laser beam as particles in an optical tweezers. Thus the optical index of the droplets is bigger than the optical index of the bulk. As the two optical indices are $n_{\text{PMMA}} = 1.49$ and $n_{\text{octanone}} = 1.415$, we conclude that the droplets are the rich phase in PMMA. Notice that this phenomenon appears when the laser is originally focused in the poor phase at less than $30 \mu\text{m}$ of the rich phase, probably because one needs a transfer of PMMA materials to create the rich droplet. If the laser is originally on a rich phase, we sometimes observe a growth of the whole rich phase after a transient state where complex phenomena appear (creating interfaces, collapsing).

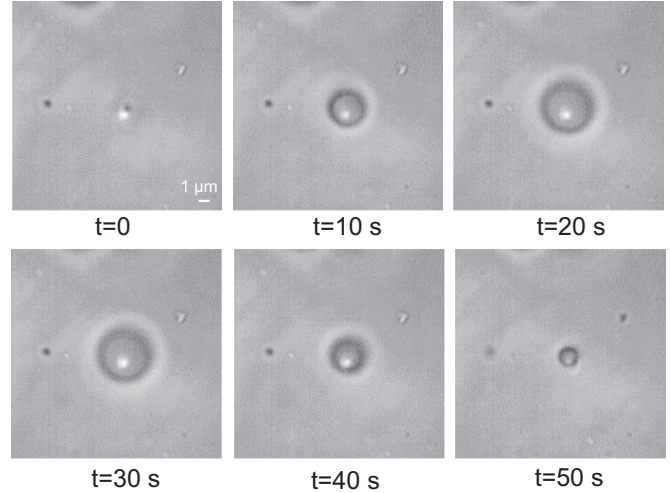


FIG. 2. Droplet oscillation. Images of the octanone-PMMA sample at a volume fraction 12.8% in PMMA at room temperature 298 K. The six images have been taken at 10 s time intervals using a microscope objective $\times 63$; the image size is $15 \mu\text{m}$. A droplet, rich in PMMA, grows for the first 30 s and then it decreases. This oscillatory phenomenon is produced by an infrared laser beam of intensity 130 mW, which is focused inside the sample by the objective. At the top left of each image, we can see an interface of another PMMA-rich phase which is at equilibrium because at this temperature, the medium is in the heterogeneous phase. The bright point is the reflection of the laser beam.

To characterize this phenomenon, we begin by measuring the growth velocity of droplets as a function of the laser power in a $\phi = 12.8\%$ sample. The oscillating droplets are acquired at 20 fps with the camera. We measure the time Δt_d needed by a growing droplet to reach an imposed diameter d . The mean growth velocity is given by $v_g = \frac{d}{\Delta t_d}$. We plot in Fig. 3 v_g as function of the laser power for two chosen diameters $d = 1.1 \mu\text{m}$ and $d = 2.8 \mu\text{m}$, for several droplets in different positions of the cell. Below 70 mW, there are no droplets. Above 420 mW, the scattering of the laser beam by the sample is too big to do a correct measurement. In the measurement region, the mean velocity v_g is well approximated by a linear function of the laser intensity, whose slope p_d is a decreasing

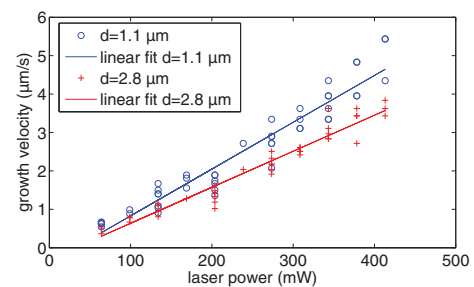


FIG. 3. (Color online) Growth velocity of the droplet in the first instants of their formation as a function of the laser power. It is measured from the time which is needed by a growing drop to reach the diameter d . The measurement is repeated on various droplets in different positions of the sample. The dispersion of the points in the plot could be due to the heterogeneities of polymer concentration in the cell.

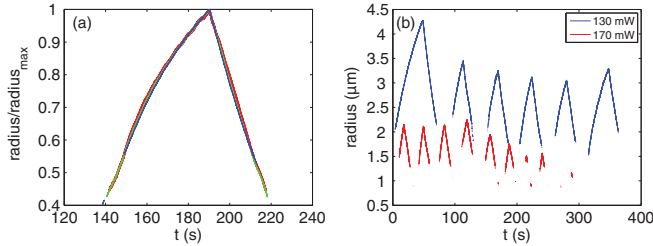


FIG. 4. (Color online) (a) Radius of PMMA-rich droplets as a function of time for different detection thresholds (red: 155, green: 160, blue: 168 in gray scale over 255) of the droplet edge in the image analysis normalized to the maximum measured radius. The collapse of all the curves ensures that the time evolution of the radius measured by this method correctly describes the droplet dynamics. The plotted data have been recorded in a sample with a PMMA volume fraction $\phi_c = 12.8\%$ (laser beam of intensity 134 mW). (b) Droplet radius as a function of time at two different powers (130 and 170 mW) of the focused laser beam. The oscillation frequency is a function of the laser power.

function of d , specifically in the figure at $d = 1.1 \mu\text{m}$, $p_d = 12.2 \mu\text{m/s/W}$, and $d = 2.8 \mu\text{m}$, $p_d = 9.4 \mu\text{m/s/W}$.

To characterize the oscillations, we implement a program with ImageJ to get the edge of the droplet in each image. We then determine the area \mathcal{A} and the radius $R = \sqrt{\mathcal{A}/\pi}$ of the droplet. As the position of this edge is sensitive to the chosen value of the threshold, we plot in Fig. 4(a) the value of the radius as a function of time for several thresholds. We check that if we rescale the curves by the maximum radius, all curves collapse. The absolute uncertainty on R is about $0.5 \mu\text{m}$, which is the diffraction limit. This method is not relevant for very small droplets because we do not get the right edge for two reasons. The first is that diffraction effects dominate. The second is that the contrast inside the droplet changes during the growth. Thus a fixed threshold cannot describe the edge of the droplet at all times. Therefore we plot in Fig. 4(b) only the dynamics for the radius above $1.5 \mu\text{m}$.

On one oscillation, we can see that the change of regime (from increase to decrease) is quite sudden. We succeeded in doing at the same spot several oscillations at two different laser intensities. Results are plotted in Fig. 4(b). An increase in laser intensity results in an increase of the oscillation frequency and a decrease of the maximum amplitude of the droplet. We tried unsuccessfully to measure quantitatively this effect, because, as we can see in Fig. 4(b), the variation of the droplet maximum radius at fixed intensity perturbs the effect. Furthermore other parameters, like local changes of concentration, dusts, and aging may disturb our measurement. Nevertheless, from our analysis at short times, we know that the larger the laser power, the faster the droplet growth.

IV. THE PHYSICAL MECHANISMS

What is the origin of this laser-induced transition? A droplet of PMMA-rich phase is initiated in the PMMA poor phase and then oscillates. Where does this PMMA accumulation come from? It can not be a simple effect of heating because this binary mixture has an UCST, so an increase in temperature

should provoke an homogenization of the solution. But a local heating creates gradients of temperature and then thermophoresis. We can estimate the increase of temperature due to the laser by measuring the absorption coefficient of the mixture in a cell at $\lambda = 1064 \text{ nm}$. To avoid light scattering, this absorption measurement is performed by keeping the cell at a temperature larger than T_c , when the sample is well mixed. This gives us an estimation of the extinction coefficient of the mixture $[\epsilon_{\text{PMMA}}] \approx 9 \text{ m}^{-1}$ and so an estimation of the temperature increase, which is about $\Delta T \approx 5 \text{ K}$ at the focal point given by the formula in Ref. [16].

A. The Soret effect

This increase should be enough to observe a thermophoretic effect. The sign of the thermophoretic coefficient (Soret coefficient) has been measured by applying a 10 K difference to a PMMA-octanone mixture at working concentration in a square cell about 5 cm high. The hot point was at the top to avoid convection effects. The temperature of the whole cell was above the critical point to avoid demixing during the experiment. After 5 days, the top of the cell was clearly less concentrated than the bottom. We performed the same experiment at a fixed temperature for the whole cell. This shows us that there is no segregation. In the range of concentration that we used in the experiment it does not change sign. In Ref. [17] they give a Soret coefficient $S_T = 0.11 \text{ K}^{-1}$ for PMMA/cyclohexanone, which is close to our PMMA-octanone mixture, and a rough estimation from our experimental setup gives us a value around $S_T = 0.1 \text{ K}^{-1}$. The positive sign of the thermophoretic coefficient (Soret coefficient) means that the PMMA is attracted to low-temperature regions. So this does not explain the first growth of the droplet, but it must be an important issue in the oscillations.

B. Laser trapping and electrostriction

The presence of the focused laser beam produces a second effect: the trapping of PMMA. We estimate the stability of this trap, taking into account that the radius of gyration of the polymer is about $\Xi_0 = 1 \text{ nm}$ [13]. At this size, we are in the Rayleigh approximation for light. We calculate the ratio between the scattering force and the gradient force on the particle [18] $\mathcal{R} = \frac{F_{\text{scatt}}}{F_{\text{grad}}}$. This ratio should be less than one to get a stable trap. We got $\mathcal{R} = 10^{-7}$. The trap is thus stable. But to trap correctly, the trapping force also needs to be bigger than the thermal forces acting on the PMMA bead. To check that, we have to estimate the Boltzmann factor $\exp(-U_{\text{grad}}/k_B T) \ll 1$ where U_{grad} is the potential of the gradient force [19]. In our case, inserting the experimental values in the equation for U_{grad} of Ref. [19] we obtain $U_{\text{grad}} \approx 5 \times 10^{-26} \text{ J}$, which is much smaller than $k_B T \approx 4 \times 10^{-21} \text{ J}$. So even if the trap is stable, the gradient force is not sufficient to trap the polymer.

Finally, the laser can induce electrostrictive forces through its electric field gradient [9]. As $n_{\text{PMMA}} > n_{\text{octanone}}$, this force results in an attraction of the polymer close to the focused laser beam through the osmotic compression of the solute.

C. Summary of the mechanisms

To summarize, the rich phase created by the laser is due to an excess of polymer brought by the laser probably by electrostrictive forces. As at this excess concentration the polymer mixture is not thermodynamically stable, the mixture separates spontaneously and the new phase grows gradually with an increasing amount of PMMA. But this effect is balanced by the thermophoretic effect which brings the polymer toward the low-temperature region. However, this simple explanation does not give us the reason of why the phase should decrease at a certain point. That needs a more precise model, which includes as activation mechanisms a combination of the above mentioned thermophoretic effects and electrostriction and their dependences in concentration of PMMA. It is important to notice that we tried the same experiments in other mixtures (for example, water-C12E5) without observing oscillations. This can be understood because the indexes of refraction of the two phases of water-C12E5 are very close and the accumulation rate produced by the beam is not enough to compensate the other effects which reduce concentration. In general, to observe oscillations in binary mixtures, a particular combination of attraction and repulsion parameters mentioned above is needed in a way that the expected concentration which balance these parameters is actually in a thermodynamically forbidden state.

V. THE MODEL

All of these physical mechanisms can be taken into account in a full model [20], which, however, has too many parameters to catch the simple physical mechanisms. Thus we describe here a simplified version which contains the main ingredient and shows that indeed local forcing may produce oscillation in a binary mixture. We start from the model developed in Refs. [11,21] to explain another type of oscillation phenomenon in phase transitions which was observed in an UCST transition during a slow cooling of a mixture [10,11]. This model is based on the Landau phase transition theory, to which a pumping term has been added [11,21]:

$$\partial_t \varphi(x,t) = \partial_x [(3\varphi^2 - 1)\partial_x \varphi] - M^2 \partial_x^4 \varphi - \xi \varphi, \quad (1)$$

where $\varphi = (\phi - \phi_c)/(\phi_0 - \phi_c)$ is the reduced volume fraction, with $\phi_0(T)$ the equilibrium volume fraction of PMMA as a function of temperature, which takes into account the critical behavior of the mixture, i.e., $\phi_o - \phi_c = \pm \sqrt{a_o(T - T_c)/b_o}$, which is equivalent to the parabola $T(\phi_o)$ used in in Sec. II to fit the data of Fig. 1. In Eq. (1) the nonlinear diffusive term $\partial_x [(3\varphi^2 - 1)\partial_x \varphi]$ and the interface term $-M^2 \partial_x^4 \varphi$ are the standard terms derived from the Landau phase transition theory. Thus, when $\xi = 0$, the equation describes the standard phase transition dynamics, where $\varphi = 1$ in the equilibrium-rich phase and $\varphi = -1$ in the equilibrium-poor phase. When $\xi \neq 0$ the term $\xi \varphi$ acts as a source term proportional to φ via a pumping coefficient ξ that in the original model of Refs. [11,21] was $\xi \propto \frac{\partial_t \phi_0}{\phi_0}$. In order to take into account the localized pumping performed by the laser in our experiment we change this term in a time-independent very localized source. Specifically we fix the amplitude $\xi = \xi_0$ in a region of size S_ξ around a specific point x_0 and 0 elsewhere. Notice

that this term models the ensemble of the above described pumping mechanisms independently of their nature, and it is used only to check whether a local pumping introduced in the Landau theory is able to produce oscillations. We solved numerically Eq. (1) for different values of ξ_0 , S_ξ , and M . The numerical integration is performed by finite difference in space, by dividing the interval $0 \leq x \leq 1$ in N points. The integration in time is performed by a fourth-order Runge-Kutta method. We checked that the results are independent of N by changing it from 50 to 400. The initial conditions are $\varphi = -1$ in all of the points of the interval. Two types of boundary conditions have been used: (1) $\varphi(0) = \varphi(1) = -1$ and (2) $\partial_x \varphi|_{x=0} = \partial_x \varphi|_{x=1} = 0$. We mostly used the first type because they correspond to have a good reservoir at the extremes, but the results do not change too much using the second. The forcing term is $\xi = \xi_0/S_\xi$ for $(x_o - S_\xi/2) \leq x \leq (x_o + S_\xi/2)$ and 0 elsewhere. Notice that there are three length

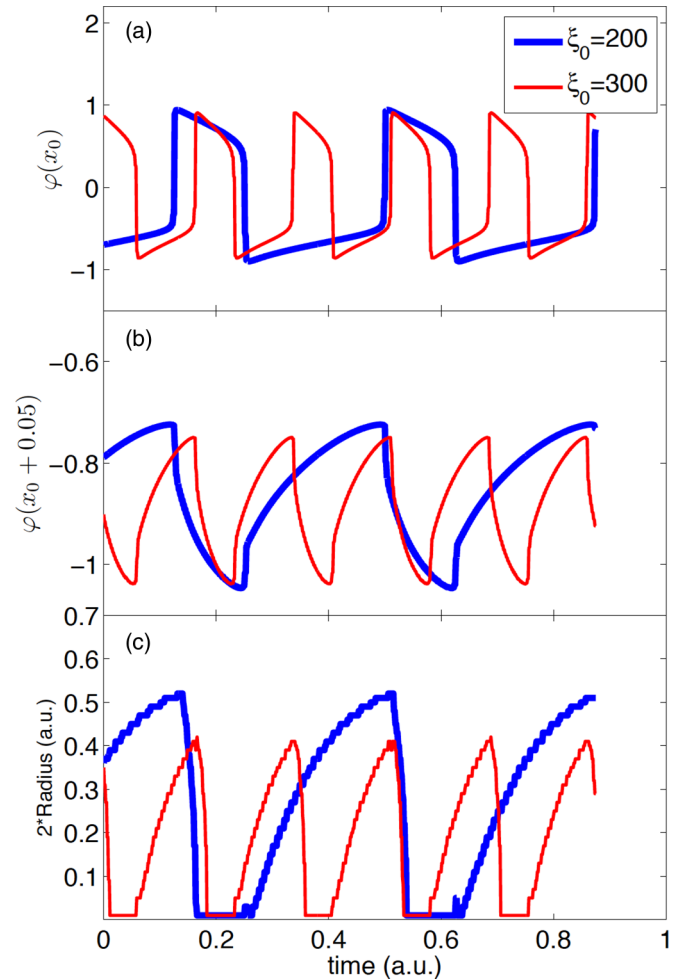


FIG. 5. (Color online) Numerical solution of Eq. (1). Mass fraction φ as a function of time, measured at the forcing point (a) and at $x_o + 0.05$ at two different values of ξ (b). Regular oscillations appear for ξ larger than a threshold value $\xi_o \simeq 1.5/S_\xi$. The bigger ξ , the faster the oscillations are. (c) Size of the PMMA-rich phase calculated numerically from Eq. (1). The size is estimated as the radius of the domain in which φ is larger than a defined threshold value, which is -0.9 here. The radius oscillations are smaller and faster when the source term is bigger.

scales in this problem: the integration domain which is set to one, the forcing size, and M . The oscillations do not appear if $M > S_\xi$. The results presented in Fig. 4 have been obtained with $N = 100$ and the first boundary conditions. More details on the numerical integration of Eq. (1) and on its physical background will be the object of a theoretical paper.

We present here the case with initial conditions $\varphi = -1$ everywhere, with $M = 0.002$ and $S_\xi = 0.01$ in the domain $0 < x < 1$ with $x_o = 1/2$. In these conditions, we observe that for $\xi_o > 1.5/S_\xi$ the local concentration oscillates in a region around the forcing point. These oscillations can be seen in Figs. 5(a) and 5(b), where we plot the value of the local concentration at x_o and at $x_o + 0.05$ for two different values of ξ_o .

Looking at Figs. 5(a) and 5(b) we see that the bigger ξ_o is the quicker and smaller oscillations are, which is in good agreement with experimental results [Fig. 4(b)]. We also observe an oscillatory creation of a rich phase in the poor one at the forcing point in Figs. 5(a) and 5(b). Following the experimental procedure we can also estimate in the numerical simulation the radius of the domain in which φ is larger than a defined threshold value, fixed, for example, at -0.9 . The results of this estimation are plotted in Fig. 5(c) where we see that the numerical model produces a time evolution of the radius, which is very similar to that of the experiment.

Thus these numerical results show that it is possible to obtain an oscillatory phase transition just adding a local pumping term, with size $S_\xi < M$, to the standard Landau theory for binary mixtures. As we have already discussed, the physical origin of this source term comes from thermophoresis and electrostriction because both effects contribute to antagonist changes of the local PMMA density. Certainly the source term in Eq. (1) is oversimplified with respect to a full model based

on the Landau theory in which we consider a local dependence on temperature and electric field of the coefficients [20]. One could eventually use the Flory-Huggins theory [8,14], which is very well suited to describe polymer-solvent interaction. However, the model presented here has the advantage of being simple and of describing the main effects. The use of a three-dimensional model will not improve the description as surface tension effects determine the drop shape, but they do not play any role as a pumping mechanism.

VI. CONCLUSIONS

In conclusion, we have presented a local oscillating phase transition induced by a focused laser beam. We have discussed the physical mechanisms producing such an effect, showing that thermophoresis and electrostriction play an important and antagonistic role. Finally we show that a simplified model, based on the Landau theory for phase transition and a local forcing, contains enough ingredients to provoke a nonlinear oscillatory behavior reproducing the main features of the experimental observations (i.e., the dependence on the pumping rate of the drop growth velocity and the complex nonlinear time evolution of the radius). With this model we do not pretend to give a full explanation of the observations but only to point out that a local pumping may produce oscillations in the framework of the Landau theory for binary mixture. A more complete model will be presented elsewhere [20].

ACKNOWLEDGMENTS

This paper has been supported by the ERC project OUTFLOCOP. We acknowledge fruitful discussions with Jean-Pierre Delville.

-
- [1] C. Hertlein, L. Helden, A. Gambassi, S. Dietrich, and C. Bechinger, Direct measurement of critical Casimir forces, *Nature (London)* **451**, 172 (2008).
 - [2] D. S. Dean and A. Gopinathan, The non-equilibrium behaviour of pseudo-Casimir forces, *J. Stat. Mech* (2009) L08001.
 - [3] S. T. Bramwell, P. C. W. Holdsworth, and J. F. Pinton, Universality of rare fluctuations in turbulence and critical phenomena, *Nature* **396**, 552 (1998).
 - [4] S. Joubaud, A. Petrosyan, S. Ciliberto, and N. B. Garnier, Experimental Evidence of Non-Gaussian Fluctuations near a Critical Point, *Phys. Rev. Lett.* **100**, 180601 (2008).
 - [5] Y. Tsori, Colloquium: Phase transitions in polymers and liquids in electric fields, *Rev. Mod. Phys.* **81**, 1471 (2009).
 - [6] R. Wunenburger, A. Casner, and J.-P. Delville, Light-induced deformation and instability of a liquid interface. I. Statics, *Phys. Rev. E* **73**, 036314 (2006).
 - [7] J. Hofkens, J. Hotta, K. Sasaki, H. Masuhara, and K. Iwai, Molecular assembling by the radiation pressure of a focused laser beam: Poly(*N*-isopropylacrylamide) in aqueous solution, *Langmuir* **13**, 414 (1997).
 - [8] D. Anders and K. Weinberg, Thermophoresis in binary blends, *Mech. Mater.* **47**, 33 (2012).
 - [9] G. P. Morriss and L. Rondoni, Definition of temperature in equilibrium and nonequilibrium systems, *Phys. Rev. E* **59**, R5(R) (1999).
 - [10] D. Vollmer, J. Vollmer, and A. J. Wagner, Oscillatory kinetics of phase separation in a binary mixture under constant heating, *Phys. Chem. Chem. Phys.* **4**, 1380 (2002).
 - [11] M. E. Cates, J. Vollmer, A. Wagner, and D. Vollmer, Phase separation in binary fluid mixtures with continuously ramped temperature, *Phil. Trans.* **361**, 793 (2003).
 - [12] K.-Q. Xia, X.-Q. An, and W.-G. Shen, Measured coexistence curves of phase-separated polymer solutions, *J. Chem. Phys.* **105**, 6018 (1996).
 - [13] C. Crauste, C. Devailly, A. Steinberger, and S. Ciliberto, Characterization of PMMA-3-octanone binary by turbidity and light scattering measurements, [arXiv:1310.6720](https://arxiv.org/abs/1310.6720).
 - [14] P. G. de Gennes, *Scaling Concepts in Polymer Physics* (Cornell Univ. Press, Ithaca, NY, 1979).
 - [15] J. R. Gomez-Solano, A. Petrosyan, S. Ciliberto, R. Chetrite, and K. Gawędzki, Experimental Verification of a Modified Fluctuation-Dissipation Relation for a Micron-Sized Particle in a Nonequilibrium Steady State, *Phys. Rev. Lett.* **103**, 040601 (2009).
 - [16] E. J. G. Peterman, F. Gittes, and C. F. Schmidt, Laser-induced heating in optical traps, *Biophys. J.* **84**, 1308 (2003).
 - [17] D. Stadelmaier and W. Keohler, Thermal diffusion of dilute polymer solutions: The role of chain flexibility

- and the effective segment size, [Macromolecules](#) **42**, 9147 (2009).
- [18] K. C. Neuman and S. M. Block, Optical trapping, [Rev. Sci. Instrum.](#) **75**, 2787 (2004).
- [19] A. Ashkin, J. M. Dziedzic, J. E. Bjorkholm, and S. Chu, Observation of a single-beam gradient force optical trap for dielectric particles, [Opt. Lett.](#) **11**, 288 (1986).
- [20] The connection of our simple and minimal model with a more physical one will be the subject of a theoretical paper where the weight of the various mechanisms will be evaluated more precisely.
- [21] J. Vollmer, G. K. Auernhammer, and D. Vollmer, Minimal Model for Phase Separation under Slow Cooling, [Phys. Rev. Lett.](#) **98**, 115701 (2007).